

Combined BC/MD approach to the evaluation of damage from fast neutrons and its implementation for beryllium irradiation in a fusion reactor

V A Borodin^{1,2}  and P V Vladimirov^{1,3} 

¹ National Research Centre 'Kurchatov Institute', Kurchatov sq. 1, 123182 Moscow, Russia

² NRNU MEPhI, Kashirskoe sh. 31, 115409 Moscow, Russia

³ Institute for Applied Materials Applied Materials Physics, Karlsruhe Institute of Technology, Eggenstein Leopoldshafen, Hermann von Helmholtz sq. 1, D 76344 Germany

E mail: borodin_va@nrcki.ru

Abstract

The determination of primary damage production efficiency in metals irradiated with fast neutrons is a complex problem. Typically, the majority of atoms are displaced from their lattice positions not by neutrons themselves, but by energetic primary recoils, that can produce both single Frenkel pairs and dense localized cascades. Though a number of codes are available for the calculation of displacement damage from fast ions, they commonly use binary collision (BC) approximation, which is unreliable for dense cascades and thus tend to overestimate the number of created displacements. In order to amend the radiation damage predictions, this work suggests a combined approach, where the BC approximation is used for counting single Frenkel pairs only, whereas the secondary recoils able to produce localized dense cascades are stored for later processing, but not followed explicitly. The displacement production in dense cascades is then determined independently from molecular dynamics (MD) simulations. Combining contributions from different calculations, one gets the total number of displacements created by particular neutron spectrum. The approach is applied here to the case of beryllium irradiation in a fusion reactor. Using a relevant calculated energy spectrum of primary knocked-on atoms (PKAs), it is demonstrated that more than a half of the primary point defects ($\sim 150/\text{PKA}$) is produced by low-energy recoils in the form of single Frenkel pairs. The contribution to the damage from the dense cascades as predicted using the mixed BC/MD scheme, i.e. $\sim 110/$

PKA, is remarkably lower than the value deduced from uncorrected SRIM calculations ($\sim 145/\text{PKA}$), so that in the studied case SRIM tends to over-predict the total primary damage level.

Keywords: irradiation, neutrons, point defects, beryllium, Monte-Carlo simulations, molecular dynamics simulations

(Some figures may appear in colour only in the online journal)

1. Introduction

The quantitative evaluation of the primary damage level in fast neutron irradiated materials is not an easy task. Though neutrons are the primary cause of the damage, the cross-section of neutron scattering on atoms of the majority of nuclear reactor structural and functional materials is low (within several barns) and the share of atoms displaced in irradiated materials by neutrons themselves is negligibly low. However, for the same reason of low scattering cross-section, the successful collisions of neutrons with target atoms are nearly head-on ones and thus the recoils get a noticeable share of the neutron kinetic energy (i.e. tens and hundreds of keV, depending on the particular neutron energy spectrum). The collision cross-section of charged energetic primary recoils (also called primary knock-on atoms (PKAs)) with the target atoms is much higher than that of neutrons and the dominant part of atom displacements in neutron-irradiated materials is normally produced by PKAs. The spectrum of initial PKA kinetic energies, dN_{PKA}/dE , can be recalculated from the known neutron spectrum $\Phi_n(E_n)$ over neutron energies E_n as [1]

$$\frac{dN_{\text{PKA}}(E)}{dE} = \int_0^{E_n^{\max}} \Phi_n(E_n) \frac{d\Sigma(E_n, E)}{dE_n} dE_n, \quad (1)$$

where E_n^{\max} is the maximum neutron energy in the spectrum, E the energy transferred to PKA, $d\Sigma/dE_n$ the neutron scattering cross-section on target atoms, and we limit ourselves to one-component targets in order to avoid cumbersome equations. Due to the kinematics of neutron scattering, in realistic neutron irradiation environments neutron flux creates in irradiated materials a wide energy spectrum of PKAs ranging from effectively zero up to E_n^{\max} reached in the head-on collisions. For the particular case of beryllium, which is used in this paper as a relevant example, we use the calculated PKA energy spectrum in the beryllium first wall of the future fusion reactor DEMO [2], where 14 MeV neutrons from (D, T) fusion reaction dominate in the neutron spectrum [3]. Figure 1 shows the normalized probability density of PKA creation in the selected neutron spectrum, p_{PKA} , recalculated from the above-mentioned PKA energy spectrum using the relation

$$p_{\text{PKA}}(E) = \frac{1}{\phi N_0} \frac{dN_{\text{PKA}}}{dE}, \quad (2)$$

where ϕ is the neutron flux and the numerical factor $N_0 = 2.14 \times 10^{20}$ recoils $(\text{n cm}^{-2})^{-1}$ is selected so as to provide the normalization condition,

$$\int_0^{E_{\max}} p_{\text{PKA}}(E) dE = 1.$$

It can be seen that while most of the primary recoils have energy less than 2 MeV with the peak at 30–50 keV, the high-energy tail extends to more than 5 MeV.

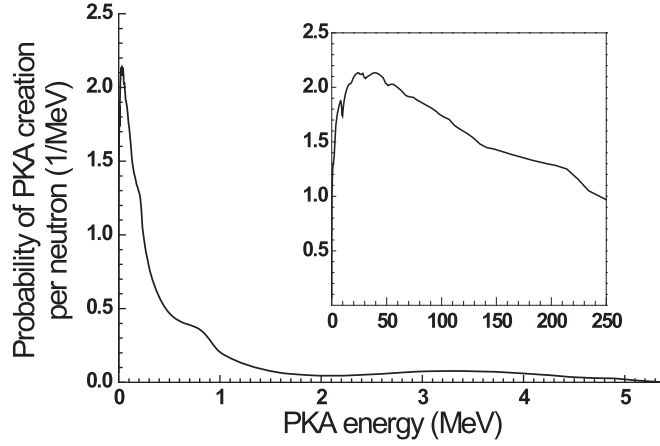


Figure 1. The probability density p_{PKA} to create primary recoils with certain energy for neutron irradiation of beryllium with the neutron flux spectrum expected on the first wall of DEMO reactor (based on the data from [2]). The insert shows the same curve in the narrower energy range (with PKA energy at abscissa measured in keV).

When the PKA energy spectrum is known, the number of atomic displacements (i.e. the total number of Frenkel pairs, G) created in a target material by neutron irradiation can be written down as [1]

$$G = \int_{E_d}^{E_{\max}} \frac{dN_{\text{PKA}}}{dE} \nu(E) dE, \quad (3)$$

where E_d is the minimum transferred energy required to irreversibly displace a target atom from its lattice site, E_{\max} the maximum energy that can be transferred to a target atom in the relevant neutron spectrum, and $\nu(E)$ is the average number of stable Frenkel pairs produced by a primary recoil ion with the initial kinetic energy E . For the case of beryllium target, the first-principles based estimates give $E_d \sim 20$ eV [4], while E_{\max} depends on the neutron spectrum (e.g. for a typical fusion spectrum with a large share of 14 MeV neutrons, $E_{\max} \approx 5$ MeV, see figure 1).

As can be seen from equation (3), in order to estimate the average rate of Frenkel pair production, one has to know two independent functions – the PKA energy spectrum and the function $\nu(E)$ for all relevant PKA energies. The calculations of PKA spectra can be done quite reliably with the modern software (e.g. FISPACT-II code [5]) and nuclear data libraries [1], so in the description below we deal primarily with the determination of the average number of displacements from PKA with different initial kinetic energies E .

The most straightforward way to determine $\nu(E)$ is to use standard analytical expressions, such as the Norgett Robinson Torrens (NRT) model [6], that relate the number of created atomic displacements to the energy, T_d , lost by the ion in the damage events. Unfortunately, in addition to the creation of displacements, fast ions have alternative channels of energy loss (electronic stopping, phonon excitation) and so T_d can be considerably lower than E (e.g. a 500 keV iron ion propagating in iron loses only roughly 200 keV of its initial kinetic energy for atom displacement [7]). Moreover, the relation between T_d and E is quite non-trivial and requires serious additional efforts for its calculation, making the use of standard analytical formulae much less simple than it might seem.

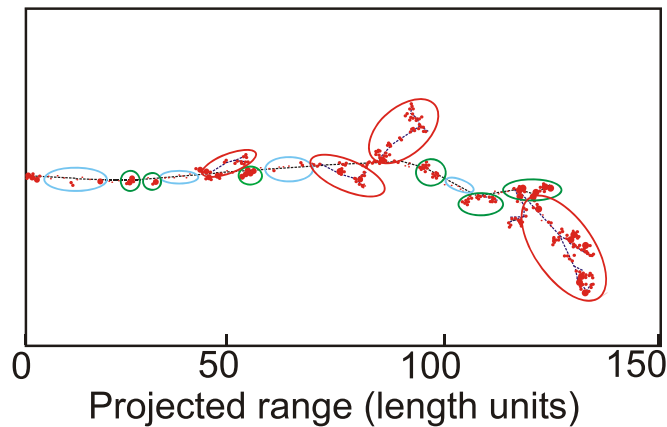


Figure 2. A sketch of a fast ion induced displacement cascade (black dot lines mark the trajectories of the ion and energetic higher order recoils). The displaced atoms are marked with red dots. Regions of Frenkel pair creation are encircled in light grey (cyan in colour version), dense localized cascades in darker grey (green), and the branches of secondary and higher order recoils in black (red).

In order to improve the estimates of the average number of displacements created by a fast ion, it is currently common to use numerical methods solving the ion transport equation. The evident advantage of the numerical approach is its ability to include in the calculation various relevant factors that affect ion propagation in the matter, such as non-damaging energy loss, sample geometry and composition, etc. The most widely used approach is based on the Monte-Carlo algorithms, the most known example being the SRIM code [8]; a recent example of the approach applying the convolution of SRIM-based estimates of $\nu(E)$ with the PKA energy spectrum created by a particular neutron spectrum can be found in [9]. In these algorithms the ion transport through the target is simulated in the framework of binary collision (BC) approximation as a sequence of fast ion collisions with individual target atoms. For each fast ion its trajectory is implemented as a stochastic realization of a Markov process. That is, the distances between the consecutive collisions are selected at random (with the average distance defined by the target density) and the ion moves straight between the collisions. The energy transferred to the target atom and the kinematics of scattering are determined according to a predefined scattering cross-section, assuming a random value of the impact parameter. In each collision, the energy of the primary ion decreases and eventually falls below $2E_d$, so that no more target atoms can be displaced. Very often, not only the primary ion trajectory is followed until it stops, but also the trajectories of the whole set of secondary and higher order recoils. Simulating in this way trajectories of sufficiently large number of primary ions with the same initial kinetic energy E , one can calculate not only the average number of irreversible displacements of target atoms, but also other useful parameters, such as the average projected ion range, scattering, etc.

An illustrative example of a fast ion trajectory is shown in figure 2. ‘Fast’ means here that the initial kinetic energy of the ion is high enough to irreversibly displace many recoiled atoms from their lattice positions. The irreversibility implies that each such recoil gets energy above a certain threshold to be able to move sufficiently far from its original location in order to avoid spontaneous recombination with the remaining vacancy. That is, the transferred energy should be at least not lower than E_d , but in more practical situations (corresponding e.g. to typical reactor operation conditions) it must be even higher because at temperatures of

practical interest too close Frenkel pairs can quickly recombine as a result of interstitial mobility. Assuming for the lower threshold the value of some tens of eV, as typical for many solids, by ‘fast’ ion we understand below ions with energies exceeding at least several keV.

As one can notice, three typical modes of damage creation can be separated depending on the energy T transferred to secondary recoil. When the transferred energy is lower than a certain threshold E_{low} , only separate single Frenkel pairs are produced. Such collision events with low energy transfers to recoil atoms are most frequent at the early stages of fast ion deceleration, when the ion velocity is still high and small-angle scattering events dominate. Note that E_{low} can be noticeably higher than E_{d} . For example, molecular dynamics (MD) based calculations for beryllium indicate $E_{\text{low}} \approx 500$ eV, in agreement with SRIM calculations showing only separate Frenkel pairs on the primary ion trajectory for Be ions with energies $T \leq 500$ eV [10]. The average number of such Frenkel pairs grows with E in this energy range, but remains somewhat lower than one would expect from the NRT equation [6].

When the energy transferred to secondary recoil exceeds E_{low} , the mode of damage production changes. The recoil displaces already multiple neighbour atoms that, in turn, displace their neighbours and thus a collective movement of many atoms within a localized volume occurs. The maximum volume of such ‘dense cascade’ can reach as much as several nanometers in diameter, but freezes down typically within a picosecond, leaving behind some displaced atoms and the equal number of unoccupied lattice positions (vacancies). According to several MD simulations, single dense cascades are created only if the ion energy does not exceed a certain threshold, E_{high} , above which well-separated dense cascades can be identified along the ion trajectory [11–13]. The numerical value of E_{high} is less certainly defined than E_{low} and can vary, depending on the particular material, from several keV to tens of keV. For example, the MD simulation results for beryllium indicate $E_{\text{high}} < 3$ keV [10], while for iron it is rather ~ 20 keV [14].

Finally, when the energy transmitted to secondary recoil exceeds E_{high} , such recoil can be considered as another ‘fast’ ion that launches its own branch of the collision cascade and thus can be treated on the same grounds as the PKA.

The main problem with the evaluation of the primary displacement damage with the help of BC codes is the treatment of dense cascades created by recoils with the energy in the intermediate range, $E_{\text{low}} < T < E_{\text{high}}$. Indeed, it is well known that in order for the BC approximation used in MC approach to be fully applicable, the distance between the consecutive collisions must be much larger than the interatomic distance so that the collisions are independent from each other. This condition is evidently violated for the secondary and higher-order recoils that get kinetic energy in the range corresponding to the ‘dense cascade’ formation. As a result, the numbers of surviving Frenkel pairs predicted in this energy range by BC codes tend to differ (typically in the direction of overestimation [7, 15]) from those obtained at the same energies in MD calculations, where the collective movement of atoms is fully accounted for [14]. Hence, it is generally preferable to use MD calculations when dealing with recoil energies falling in the ‘dense cascade’ range.

In contrast, in the low-energy part of the transferred energy spectrum, the average number of created point defects predicted by BC and more detailed MD simulations is very similar, provided the Monte-Carlo BC code employs a displacement threshold energy relevant for the particular interatomic potential applied in MD. Though sounding obvious, the latter requirement is not so easy to fulfil because of both the basic problems in the identification of the appropriate threshold displacement energy by numerical modelling [16] and the sensitivity of MD predictions to the employed empirical interatomic potential. For example, MD estimates of E_{d} in beryllium with two different interatomic potentials give the values of

~ 17 eV [4] and ~ 40 eV [17], while the first principles estimates indicate it to be rather ~ 30 eV [4].

The main problem one meets when applying the MD approach to the estimation of damage is its inability to treat ions with the energies well above E_{high} . In order to illustrate it, it is instructive to look at cascades in iron, possibly the most thoroughly investigated metal by now [7, 13, 18, 19]. In order to simulate the cascades with the initial iron recoil energy of 20 keV one needs simulation cells of ~ 0.5 million atoms [7]. The accumulation of reasonable damage statistics (at least 10 cascades with different initial recoil momentum orientations) for such simulation cells is a tough, but practically achievable task on modern supercomputers. On the other hand, to simulate a cascade created by 200 keV recoil, one needs already ~ 10 20 million atom cells [7], where the accumulation of relevant statistics requires quite serious efforts [7, 20]. One can find in the literature single examples of even more demanding calculations (with simulation cells of up to 500 million atoms and primary recoil energies up to 500 keV [21]), but these consume significant computer resources and present serious difficulties in the intermediate data storage, processing and visualization. Having in mind the electronic energy loss, which is quite strong at such ion energies (though only seldom directly included in MD calculations, see e.g. [20, 22]), the 200 keV MD cascade energy in terms of the created displacements should roughly correspond to PKA with the energy of ~ 0.5 MeV [7], or the medium PKA energy for 14 MeV neutron irradiation of iron-based targets in a fusion facility. For the higher recoil energies needed to describe the PKA energy spectrum part above the medium value, MD calculations are at present unrealistic. For metals noticeably lighter than iron, with more extended cascades and higher maximum PKA energies, the problems of using MD for the direct calculation of damage from high energy recoils become only more severe.

Having in mind that in the case of fast neutron irradiation the majority of PKAs have energies higher than the above-mentioned typical values of E_{high} , the development of a simulation strategy that combines the strong sides of both BC and MD approaches for the calculation of the cascade function is definitely of immediate practical value. In this paper we describe a possible implementation of such a strategy and its application to the evaluation of the level of primary damage in beryllium first wall of a fusion reactor.

2. A combined BC/MD technique of primary damage evaluation

2.1. Monte-Carlo part

In order to improve the estimates of the primary damage level predicted in the framework of the BC approximation, we follow the idea to combine BC Monte Carlo and MD calculations, as suggested in [23]. In our approach, the average number $\nu(E)$ of Frenkel pairs generated by primary recoil with the initial energy E is written down as a sum of three terms,

$$\nu(E) = \nu_1^l(E) + \nu_1^m(E) + \nu_1^h(E), \quad (4)$$

where ν_1^l , ν_1^m , and ν_1^h are the numbers of Frenkel pairs created by secondary recoils with the transferred energies in the ranges $T < E_{\text{low}}$, $E_{\text{low}} < T < E_{\text{high}}$ and $E_{\text{high}} < T$, respectively.

The number of point defects from low-energy secondary recoils, ν_1^l , is reasonably well described in the BC approximation, as already discussed in section 1, and thus can be directly evaluated applying a BC code. For the recoils that receive energy T in the intermediate range, we calculate only the numbers of such secondary recoils and use for each T an average number of defects $\nu_{\text{MD}}(T)$ calculated independently using MD. The formal relation for ν_1^m can be written down as

$$\nu_1^m(E) = \int_{E_{\text{low}}}^{E_{\text{high}}} [S_2(E, T) + W_1(E, T)] \nu_{\text{MD}}(T) dT, \quad (5)$$

where $S_2(E, T) dT$ is the average number of secondary recoils in the energy range $(T, T + dT)$ created by fast ions with energy E and W_1 is the probability density that a decelerating fast ion acquires the energy T after the collision that makes its kinetic energy fall below E_{high} . The term with W_1 in equation (5) takes into account that in the typical neutron irradiation conditions the recoil range is much less than the size of irradiated sample and thus one has to add to S_2 also the contribution from the dense cascades created by the primary recoils at the end of their ranges. Strictly speaking, when PKA energy falls below E_{high} , it may at the same time fall below E_{low} as well. In this case it should be added rather to $\nu_1^l(E)$, but, as will be shown below, the contribution of such PKAs to the total number of defects is negligible.

Finally, the number of Frenkel pairs created by the ‘fast’ secondary recoils can be written down as

$$\nu_1^h(E) = \int_{E_{\text{high}}}^{T_{\text{max}}} S_2(E, T) \nu(T) dT, \quad (6)$$

where T_{max} is the maximum energy that the primary recoil with energy E is able to transfer to a target atom (in the case of one-component target, as considered here, $T_{\text{max}} = E$). When writing equation (6), we have taken into account that high-energy secondary recoils in a one-component target are of the same type as the primary recoil and thus the number of defects created by them is described by the same function $\nu(T)$. In other words, equation (4) is essentially an integral equation for ν .

Due to the specific nature of the cascade, the simplest way to solve this integral equation is to use recursion. Indeed, for each high-energy secondary recoil the function ν is again expressed in terms of equation (4) and then substituted into equation (6), giving

$$\nu(E) = \nu_2^l(E) + \int_{E_{\text{low}}}^{E_{\text{high}}} S_3^m(E, T) \nu_{\text{MD}}(T) dT + \int_{E_{\text{high}}}^{T_{\text{max}}} S_3^h(E, T) \nu(T) dT, \quad (7)$$

where ν_2^l is the total number of isolated Frenkel pairs directly created by the primary ion and all ‘fast’ secondary recoils in low-energy-transfer collisions, that is

$$\nu_2^l(E) = \nu_1^l(E) + \int_{E_{\text{high}}}^{T_{\text{max}}} S_2(E, T) \nu_1^l(T) dT; \quad (8)$$

the integral in the second term of equation (7) gives the total number of point defects created by the second and the third generations of recoils that have got the energy in the intermediate range, with the kernel

$$S_3^m(E, T) = S_2(E, T) + W_1(E, T) + \int_{E_{\text{high}}}^{T_{\text{max}}} S_2(E, T') [S_2(T', T) + W_1(T', T)] dT' \quad (9)$$

and the third term in equation (7) describes the number of defects created by the high-energy recoils of the third generation, with

$$S_3^h(E, T) = \int_T^E S_2(E, T') S_2(T', T) dT'. \quad (10)$$

It is clear that the fraction of the third-order ‘fast’ recoils, as determined by function S_3^h , for any primary recoil is notably less than the number of second-order ‘fast’ recoils and thus the contribution to the total number of generated defects from the last term in equation (7) is less than that from the last term in equation (4). Repeating the recursion procedure again and

again, one gets at the k th recursion level ($k \geq 3$) the equation

$$\nu(E) = \nu_k^1(E) + \int_{E_{\text{low}}}^{E_{\text{high}}} S_{k+1}^m(E, T) \nu_{\text{MD}}(T) dT + \int_{E_{\text{high}}}^{T_{\text{max}}} S_{k+1}^h(E, T) \nu(T) dT, \quad (11)$$

where functions ν_k^1 and S_{k+1}^m are determined recursively from

$$\nu_k^1(E) = \nu_{k-1}^1(E) + \int_{E_{\text{high}}}^{T_{\text{max}}} S_k^m(E, T) \nu_{k-1}^1(T) dT, \quad (12)$$

$$S_{k+1}^m(E, T) = S_k^m(E, T) + \int_{E_{\text{high}}}^{T_{\text{max}}} S_k^h(E, T') [S_2(T', T) + W_1(T', T)] dT' \quad (13)$$

and

$$S_k^h(E, T) = \int_T^{T_{\text{max}}} S_{k-1}^h(E, T') S_2(T', T) dT'. \quad (14)$$

The unknown last term in equation (11) is determined by the number of high-energy recoils of consecutively higher generation order. In practice, each branching of cascade sharply reduces the number of next-generation ‘fast’ recoils, so that the unknown term quickly vanishes as k increases and the recursion sequence stops at a finite iteration stage K , giving

$$\nu(E) = \nu_K^1(E) + \int_{E_{\text{low}}}^{E_{\text{high}}} S_{K+1}^m(E, T) \nu_{\text{MD}}(T) dT. \quad (15)$$

As can be seen, in order to estimate the total number of displacements one needs to know only the functions ν_k^1 and S_{k+1}^m that can be determined using an appropriate BC code and the function ν_{MD} obtained from MD calculations.

Strictly speaking, the recursive procedure for the determination of the total numbers of defects created by low-energy recoils, as well as the numbers of secondary and higher-order recoils with the initial energies in the intermediate range, can be very straightforwardly implemented in any BC MC code. To do this, such a programme has to be supplemented with a tool for on-the-fly analysis of the new recoils, where the recoils with $T < E_{\text{low}}$ directly contribute to the estimate of the primary damage, whereas the recoils with the energy in the intermediate energy range add to the summary energy spectrum S^m and are not followed further. The high-energy recoil branches are to be processed according to the same procedure until they are expired. Finally, each high-energy recoil trajectory is traced only until the recoil energy falls below E_{high} , rather than below $2E_d$, while the recoil’s eventual contribution to either the isolated defect number or to the medium-energy recoil spectrum is determined depending on its final energy. Repeating this separation procedure for many primary ions with the same initial energy E , it is easy to get the energy distributions for $\nu^1(E)$ and $S^m(E, T)$ averaged over many cascades.

Unfortunately, in order to implement this procedure, one has to modify the existing MC codes, which implies the access to the source code. An alternative approach, followed in this paper, is to post-process the information about all collisions saved in the output files of the available MC codes. The strong disadvantage of this approach is the very large size of files required for saving the output. At the primary recoil energies of hundreds of keV and quite a modest statistics (say, only 100 attempts for the same initial recoil energy), the output file sizes can reach many gigabytes. To overcome this problem, only the data for the limited number of recoil generations can be saved. For example, the widely used SRIM code saves the data for only the second- and (partly) third-generation recoils. However, this is rarely

sufficient for fast neutron irradiation that creates quite a number of very energetic PKAs and, as a result, a lot of fast recoils remains in the recoil energy spectrum of even the third recoil generation. Hence one additionally meets the need to estimate the contribution of these remaining fast recoils to the overall damage.

In order to do it, we use an indirect recursion. That is, the spectra $S_3^m(E, T)$ are directly evaluated for ions with energies E on some energy grid between E_{high} and E_{max} from the BC code output data and are then used for the numerical integration of the recursion relations (12) (14). The largest body of calculation here is required for the evaluation of all the necessary spectra, especially when E_{max} is high and the ion kinetic energy grid used for MC runs is sufficiently dense. On the other hand, the numerical evaluation of recursion equations converges quickly. The reason is that the collisions with high energy transfers are very rare and thus the maximum energies T_{max} of secondary and higher order recoils generated by PKA with the initial energy E are remarkably less than E , being the lower, the higher is the recoil generation order. Correspondingly, the integration ranges in the last terms of equations (12) and (13) quickly shrink after each iteration, eventually vanishing completely.

In practical calculations, where the PKA spectrum for a desirable neutron spectrum is usually evaluated prior to the damage calculations, it is technically convenient to first average the relevant values over the neutron spectrum,

$$\bar{\nu}_k^1 = \int_{E_d}^{E_{\text{max}}} p_{\text{PKA}}(E) \nu_k^1(E) dE \quad (16)$$

and

$$\bar{S}_k^m(T) = \int_T^{E_{\text{max}}} p_{\text{PKA}}(E) S_k^m(E, T) dE, \quad (17)$$

where p_{PKA} is the normalized probability density of PKA creation in the selected neutron spectrum, see equation (2).

Then it is possible to write down the recursion equations averaged over the neutron spectrum, e.g.

$$\bar{\nu}_k^1 = \bar{\nu}_{k-1}^1 + \int_{E_{\text{high}}}^{E_{\text{max}}} \bar{S}_k^m(T) \nu_1^1(T) dT, \quad (18)$$

etc, and only then apply the numerical integration in order to avoid making it for each value of E .

2.2. MD part

MD is the numerical technique usually considered as the most relevant one for the modelling of dense cascades, where the primary damage is created as a result of strongly correlated atomic motion [7]. The main reason for that is generally assumed to be the fact that the size and evolution time scales of such cascades are compatible with the simulation cell sizes and calculation times achievable for MD calculations on sufficiently powerful modern supercomputers. However, this claim should be faced with a certain caution. To better understand it, let us briefly discuss the sequence of dense cascade collision stages.

In very general terms, four stages of the cascade-induced damage evolution, strongly different in the involved time scales, can be identified [7, 19], including (i) ballistic damage creation, (ii) correlated recombination, (iii) escape of mobile point defects to the bulk and (iv) the evolution of remaining immobile defects (if any) as a result of interaction with freely-migrating point defects.

The shortest stage (that lasts typically one picosecond) is the ballistic one, where the energy of the initial recoil is redistributed between the nearby atoms in the simulation cell. The number of moving atoms grows fast and then quickly decreases as the introduced energy is scattered in the surrounding matrix by both thermal conductivity and elastic waves. Due to the fast cooling down of the excited region, not all the atoms have time to return to the lattice sites and some of them remain dissolved in interstitial positions and an equivalent number of lattice sites remains unoccupied. Due to the very short duration of the ballistic stage, MD simulations can often be undertaken for the impact energies well above E_{high} and hence MD can be also used to evaluate the value of E_{high} as the highest initial ion energy for which the collision cascades mostly remain to be dense and do not break into well separated sub-cascades created by secondary recoils.

Crystal defects that remain in the cascade area after the ballistic stage termination are very different in terms of their mobility. The most mobile defects are usually single self-interstitials and, in some materials, small interstitial clusters that manifest relatively fast diffusion at the temperatures of interest for relevant applications. On the contrary, vacancies and small vacancy clusters are considerably slower, while the mobility of clusters with more than three vacancies, even if non-zero, is seldom of practical relevance. As a result, at the second stage of cascade evolution the dominant process is the diffusion of interstitial defects, a part of which recombines with nearly immobile (at these time scales) vacancy defects and another part escapes to the surrounding bulk material, becoming so called ‘freely migrating’ interstitials that further contribute to the secondary damage kinetics and are thus of the primary practical interest. Because of the correlated spatial distribution of vacancies and interstitials in the area occupied by the cascade and the relative immobility of vacancies, the recombination loss of interstitials is determined by the defect spatial distribution geometry rather than the temperature and can constitute a noticeable part of defects produced at the ballistic stage. MD simulations at the post-ballistic stage are not frequently reported because they require very long simulation runs (up to nanoseconds) even when the accelerated MD techniques are applied (e.g. the increase of simulation temperature to accelerate the interstitial diffusion). In particular, for beryllium such MD simulation was undertaken in [10], where less than a half of interstitials created at the ballistic cascade stage was shown to survive correlated recombination and escape into surrounding volume following numerical annealing at 600 K.

The third stage of cascade evolution, involving the dissolution of the non-recombined vacancies in the bulk, can hardly be done with the help of MD but can be studied, if needed, by alternative atomistic techniques, such as kinetic Monte-Carlo. Such simulations do not change the total number of surviving vacancies, but allow estimating how many vacancies eventually escape the cascade area to become freely migrating defects and which share of vacancies becomes immobilized in vacancy clusters, which should be further treated as void nuclei in the framework of more macroscopic treatment, such as the chemical rate theory [24, 25].

A common trend of the MD simulations in various metals is the power law dependence of the calculated number of defects $\nu_{\text{MD}}(E)$ on the initial recoil energy E [7], that is

$$\nu_{\text{MD}}(E) = \alpha_{\text{MD}} E^p, \quad (19)$$

where α_{MD} and p are numerical factors. The value of p is typically not much different from unity. Specifically for cascades in Be, $p = 1$ [10], though values less than one are more common (e.g. $p = 0.75$ for iron in the dense cascade energy range of 1–20 keV [7]). The prefactor values are $\alpha_{\text{MD}} \cong 18.6 \text{ keV}^{-1}$ for the post-ballistic output and $\alpha_{\text{MD}} = 8.3 \text{ keV}^{-1}$ for the case, when the material temperature allows the correlated recombination [10], assuming that E is expressed in the units of keV. When equation (19) reduces to the linear

dependence, the contribution of recoils in the dense cascade energy range to the overall number of generated point defects, entering equation (10), acquires especially simple form,

$$\nu^m = \alpha_{MD} N^m \bar{E}, \quad (20)$$

where N^m is the total number of recoils falling in the ‘dense cascade’ energy window,

$$N^m = \int_{E_{low}}^{E_{max}} \left[\int_{E_{low}}^{E_{high}} S_{K+1}^m(E, T) dT \right] p_{PKA}(E) dE \quad (21)$$

and \bar{E} is the neutron spectrum averaged energy transferred to all recoils belonging to the medium energy range,

$$\bar{E} = \frac{1}{N^m} \int_{E_{low}}^{E_{max}} \left[\int_{E_{low}}^{E_{high}} T S_{K+1}^m(E, T) dT \right] p_{PKA}(E) dE. \quad (22)$$

To conclude this section, let us briefly discuss the reliability of MD predictions. It is well known that the accuracy of MD simulations is sensitive to the reliability of the interatomic potentials used. It is important that employed potentials are able to correctly describe the effects crucial for the studied task.

When dealing with the simulation of dense collision cascades, the predictions for the ballistic stage are usually only weakly sensitive to the form of the potential. The main mode of atom interactions at this stage is the repulsion between quickly moving atoms coming close together and it is a usual practice to include in the potentials applied for cascades simulations a short-range term in the form of the universal ZBL potential [8], which dominates in close collisions. On the contrary, at the second stage of the cascade annealing the most important potential feature is its ability to correctly describe the shape and mobility of interstitials and small interstitial clusters. For example, interstitials should move much faster than vacancies and the interstitial clusters should not demonstrate unphysical features (e.g., there should be no quick artificial one-dimensional cluster diffusion if it is not expected for the studied material). For beryllium, this condition is satisfied e.g. by the potential suggested in [26], which correctly describes vacancy interactions at short separations, the ground state interstitial configuration and the diffusion modes of self-interstitials in beryllium, as predicted by first principles calculations [27, 28].

2.3. Combined BC/MD algorithm

The combined BC/MD algorithm for the calculation of the primary radiation damage that follows theoretical considerations described in two previous sections can thus be summarized as follows.

- (i) The calculation of the expected PKA energy spectrum for the particular neutron irradiation environment. Even though this information is required mostly on stage (v) below, one has to realize how large the maximum expected PKA energy is.
- (ii) The estimation of the borders of the medium-energy window, E_{low} and E_{high} . The estimates can be obtained either in BC approximation or from MD simulations. Even better might be to make a quick estimate using a BC code and then to perform several trial MD calculations to verify the BC estimates. Strictly speaking, the selection of both E_{low} and E_{high} is to some degree uncertain because neither can be defined rigorously, but it is important to select them so that only well-separated single Frenkel pairs were created at PKA energies below E_{low} and that separation into dense subcascades was sufficiently pronounced above E_{high} .

- (iii) Calculation of fast ion propagation in the studied material using an appropriate BC code. Calculations are performed for a reasonably dense discrete set of ion energies in the range corresponding to ‘fast’ ions (that is, from E_{high} to E_{max}), executing sufficient number of runs for each considered energy to achieve reasonable statistics. Strictly speaking, damage from PKAs with energies below E_{high} can be calculated as well, directly contributing to $\bar{\nu}^1$ and the energy spectrum of medium-energy recoils, but for realistic neutron spectra these contributions can be safely neglected.
- (iv) Numerical processing of the second- and higher-order recoil data in order to extract the trajectory averaged numbers of isolated Frenkel pairs and the energy spectra of second- and higher-order recoils getting the initial energy in the medium-energy range. Ideally, this processing should be done on-the-fly at stage (iii) in order to save computation time and avoid data storage limitations. If this is impossible, the relevant data should be extracted by post-processing of the ‘raw’ output files containing the data on the deceleration and scattering of PKAs and the higher-order recoils they generate. Having in mind the amount of information to be processed in this way, the post-processing requires appropriate computer utilities to perform all necessary calculations.
- (v) The calculation of the PKA energy spectrum averaged values for the Frenkel pair numbers from the low-energy recoils and the histograms of energy distribution of recoils falling in the medium-energy range.
- (vi) MD based estimation of the dependence of the function ν_{MD} on the initial recoil energy in the energy range leading to the formation of dense cascades. This is usually a formidable task in itself, but can be done only once for each particular material and is completely independent of BC calculations.
- (vii) The final calculation of point defect production numbers using the energy spectra for medium-energy recoils obtained in stage (v) and the efficiency of damage production for medium-energy recoils calculated at stage (vi).

3. An example of primary damage calculation in beryllium for a particular PKA energy spectrum

As an example of implementation of the algorithm described in section 2 for a practical case, we have applied it to evaluate the damage level expected in beryllium first wall in the future fusion reactor DEMO. The relevant PKA energy spectrum for this application was taken from [2]; see equation (1) with the normalized PKA energy spectrum $p_{\text{PKA}}(E)$ shown in figure 1. The spectrum peak lies at 30–50 keV, implying that in the case of beryllium irradiation in a fusion reactor the absolute majority of PKAs can be considered as ‘fast’.

Having in mind already mentioned results of MD simulations of cascades in beryllium [10], the borders of the medium-energy window were selected as $E_{\text{low}} = 0.5$ keV and $E_{\text{high}} = 3.5$ keV.

The BC part of the programme was implemented using the code SRIM-2013, in spite of its restrictions described above. The Be ion trajectories in beryllium were determined for ion initial energies in the range of 4 keV–5.62 MeV using a variable spacing energy grid. The used energy grid step was 1 keV from 4 to 30 keV, then 5 keV from 30 to 100 keV, 10 keV from 100 keV to 2.6 MeV, and 20 keV for the remaining energy range above 2.6 MeV. For each energy group, the data for 100 different normal incidence trajectories were calculated in the full cascade regime.

The post-processing of the data was performed using a homemade computer utility, which implements stages (iv) and (v) of the algorithm described in section 2.3. The

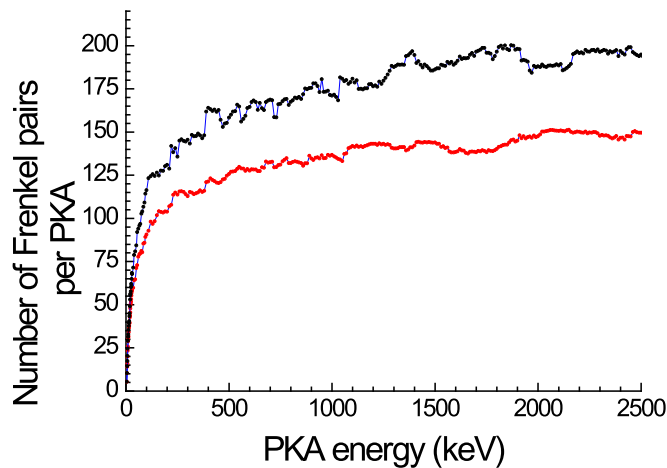


Figure 3. The numbers of single Frenkel pairs generated by PKAs only (lower red curve) and by PKAs and the secondary fast recoils together (upper blue curve) versus PKA energy.

programme reads the data from the files COLLISON.TXT produced by the SRIM code, processes the data contained in these files (in batch processing mode), extracting for each saved ion trajectory the numbers of isolated Frenkel pairs and the energy spectra of second- and higher-order recoils, averages the obtained data over all trajectories saved in each input file and eventually creates for each input file an output file with the summary information that includes the energy-dependent histograms for the numbers of isolated defects in the low energy-range and the numbers of recoils in the intermediate and fast energy ranges. The histogram that covers ‘fast’ energy range is normally not empty after this processing because SRIM does not save complete scattering data for the recoils other than the secondary ones. The information for the sum total of isolated point defects collected in the low-energy range is saved as well.

Based on these data, figure 3 compares the contributions from PKAs and the ‘fast’ secondary recoils to the direct generation of Frenkel pairs in collisions with the low energy transfer. It can be easily noticed that though isolated Frenkel pairs are mostly produced by PKAs themselves, the contribution of secondary recoils is non-negligible at all considered energies. The contributions from the third- and higher-order recoils to the isolated Frenkel pair production are not saved in SRIM output and thus cannot be analysed directly.

Quite a number of secondary recoils with the energy exceeding E_{high} are produced by PKAs with high initial energies, especially in the MeV range, as can be seen in figure 4. Even having in mind noticeable data scatter due to insufficient statistics, it can be noticed that perceptible numbers of ‘fast’ secondary recoils per PKA are observed only for recoil energies below 20–25 keV, even when the considered PKA energies reach 5 MeV. The tail of single events with higher transferred energies extends to ~ 80 keV and only very rare recoils with transferred energy above 80 keV were recorded in the processed MC output. In the ‘fast’ third-order recoil spectrum, the numbers of recoils per PKA reduce much stronger, but do not vanish completely and occasional recoils with energies up to 80 keV are still created by PKAs in the MeV range. Each such recoil can produce noticeable numbers of point defects, so it is not *a priori* evident that the contribution of the remaining ‘fast’ third-order recoils can be neglected.

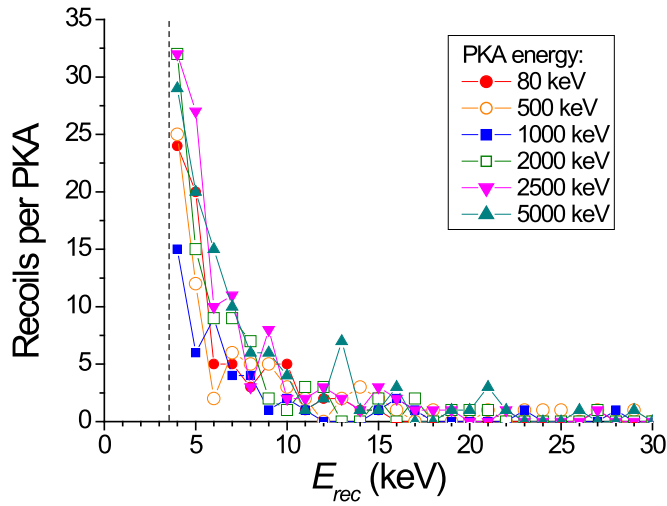


Figure 4. High energy spectrum part for the secondary recoils created by PKAs of different energies (normalized per one PKA). The PKA energies for each curve are explained in the legend. The vertical dashed line marks the lower border of the high energy region (i.e. E_{high}).

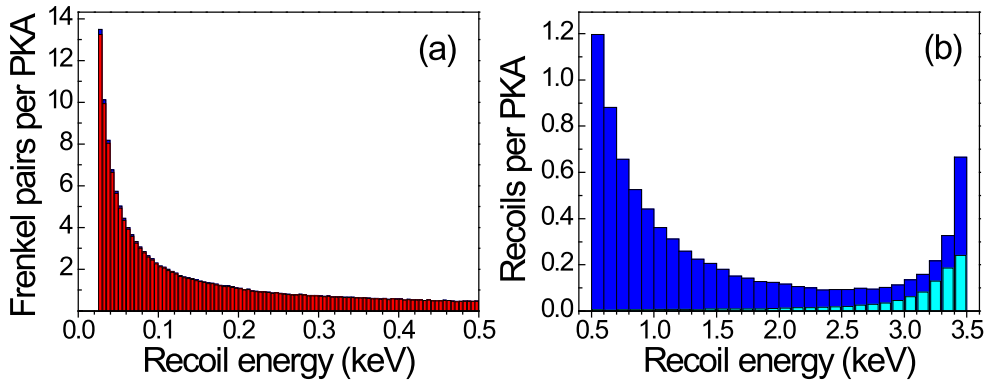


Figure 5. The final histograms for the energy distribution of isolated Frenkel pairs in the low energy range (a) and the recoil spectrum in the medium energy range (b). The lighter (light blue in colour version) columns in panel (b) show the contribution to the spectrum from decelerating PKAs.

In order to correctly evaluate the contribution of the ‘fast’ part of the recoil spectrum, all the energy spectra were integrated over the PKA energies with the weights corresponding to the selected PKA energy spectrum, shown in figure 1, and then the numerical procedure of indirect recursion described at the end of section 2.1 was applied. The final neutron spectrum averaged results for the BC part of calculations are shown in figure 5.

Figure 5(a) illustrates the sensitivity of the isolated Frenkel pair production to the recoil energy for recoils of all generations that have obtained kinetic energies below E_{low} . As can be noticed, the defect production efficiency strongly falls as the energy transferred to recoil increases. Summing all the contributions, the spectrum averaged number of isolated Frenkel pairs is evaluated to be ~ 150 per PKA.

Figure 5(b) shows the resulting energy spectrum of recoils of all generations, including PKAs themselves, falling in the medium-energy window. The total number of recoils is $N^m = 8.3$ per PKA. The relative share of recoils with certain energy decreases with the increase of the energy transferred to recoils. The exception is, however, the region close to E_{high} , where one notices an increase due to the slowing down PKAs that enter the medium energy region from the higher-energy side. As can be noticed, the share of PKA with the final energy E_{fin} (shown with light blue columns in figure 5(b)) quickly decreases as E_{fin} changes from E_{high} down to E_{low} . The share of PKAs ending their propagation with $E_{\text{fin}} < E_{\text{low}}$ is very low ($\sim 1.3\%$) and their contribution to the Frenkel defect production (0.013 per PKA) is absolutely negligible.

In order to estimate the contribution to the overall number of Frenkel pairs from dense cascades, we use the results of MD modelling of cascades in beryllium, presented in [6]. Having in mind the linear dependence of the number of Frenkel pairs on the MD cascade energy in the range of 0.5–3 keV, we can apply for the estimates equation (20), where the average energy over the medium-energy range estimated from the data shown in figure 5(b) is $\bar{E} = 1.57$ keV. Using the estimated values of N^m and \bar{E} and $\alpha_{\text{MD}} = 8.3 \text{ keV}^{-1}$ (as expected for fusion reactor relevant temperatures [10]), one easily obtains the number of Frenkel pairs produced in dense cascades to be ~ 110 per PKA. That is, dense cascades produce in beryllium noticeably less point defects as compared to the number of isolated Frenkel pairs. It should be kept in mind, however, that the relative share of defects produced in dense cascades is sensitive to the particular material and the statement above not necessarily holds true for heavier materials because dense cascades in low and high mass metals demonstrate quite different behaviour.

For comparison, the PKA energy spectrum averaged value of the Frenkel pair number obtained by using the uncorrected vacancy/recoil numbers predicted by SRIM is ~ 295 per PKA. Having in mind that ~ 150 Frenkel pairs per PKA are produced as isolated defects in low-energy-transfer collision events, it can be concluded that roughly a half of displacements is due to the secondary and higher-order recoils that launch dense cascades. According to the combined BC/MD model, the contribution of dense cascades is noticeably more modest. However, the overall difference in the predicted damage (295 displacements/PKA from SRIM versus 260 displacements/PKA from BC/MD model) is only $\sim 15\%$, which is not critical. Such relatively low difference seems to be related to very narrow energy range of recoils leading to dense cascades ($E_{\text{high}} - E_{\text{low}} < 3$ keV [10]). As already mentioned above, in heavier materials with much broader ‘dense cascade’ window such a relation not necessarily holds true.

To conclude this section, we should mention that though here we are reporting our findings for beryllium only, the approach seems to be equally applicable to other materials (e.g. multicomponent and not necessary metallic) and opens a way of calculating the damage from very energetic projectiles (including those creating damage in volumes beyond the current capabilities of MD) and making calculations faster by restricting conventional MD calculations only to those recoil energy ranges, where such calculations are practical and statistically reliable. Moreover, the approach makes it possible to express the primary damage not in terms of abstract ‘displacements’, but in terms of particular point defects and point defect clusters. Finally, by taking into account the correlated recombination in the cascade region, which can be studied by extended MD or kinetic MC, it is possible to extract from the total numbers of produced defects only the shares of ‘freely-migrating’ ones, thus automatically accounting for the ‘cascade efficiency’ factor in the damage calculations. Ideally, this would provide extended input for large-scale object kinetic Monte Carlo and rate theory models describing secondary microstructural changes in irradiated materials.

4. Conclusions

1. The paper applies a mixed BC/MD algorithm of evaluating the level of primary damage production in fast neutron irradiated materials using the information about the target PKA energy spectra in particular irradiation conditions. The approach provides a correction to the predictions of the commonly used BC codes through the application of the results of more appropriate MD calculations for defect production in dense collision cascades. In this way, the implemented approach employs the advantages of both BC and MD methods, compensating at the same time for their shortcomings. For example, it suggests a way to avoid the damage calculations by MD for high-energy PKAs, which are currently quite challenging or even impossible. It should be kept in mind, however, that the approach still requires detailed validation and verification on different materials, in order to justify its applicability as a generic methodology that works.
2. As a first step of such validation procedure, the algorithm was applied for the calculation of rates of point defect production in a particular case of beryllium irradiated by neutrons with the energy spectrum expected for the first wall of the future fusion reactor DEMO. It is shown that the total number of created displacements can be tentatively divided in two parts, namely the displacements created in low-energy-transfer collision events, which can be reliably calculated using BC approximation, and those originated from medium-energy recoils that launch dense cascades. This second contribution is demonstrated here to be quite sensitive to the way it is estimated (directly in the BC code or using the information inferred from MD). In a particular case of beryllium irradiated with the DEMO first wall neutron spectrum, MD-based estimates predict nearly 40% less damage production than expected from SRIM calculations. However, the difference in the total defect production is noticeably weaker because dense cascades produce less than a half of the total displacements.

Acknowledgments

The work was carried out using computing resources of the federal collective usage centre "Complex for simulation and data processing for mega-science facilities" at NRC 'Kurchatov Institute' (<http://ckp.nrcki.ru/>) (Russia) and HC3 computing cluster of Steinbuch Computing Centre at KIT (Germany). The funding from KIT in support of guest scientist visits to KIT, as well as support from the 5/100 Program of NRNU MEPhI are acknowledged by VAB.

This work has been carried out within the framework of the EUROfusion Consortium and has received funding from the Euratom research and training programme 2014–2018 under grant agreement No. 633053. The views and opinions expressed herein do not necessarily reflect those of the European Commission.

ORCID iDs

V A Borodin  <https://orcid.org/0000-0002-2928-0849>

P V Vladimirov  <https://orcid.org/0000-0003-2358-6043>

References

- [1] Vladimirov P and Bouffard S 2008 *C. R. Phys.* **9** 303–22

- [2] Gilbert M R, Sublet J C and Forrest R A 2015 Handbook of activation, transmutation, and radiation damage properties of the elements simulated using FISPACT II & TENDL 2014; Magnetic Fusion Plants *Tech. Rep.* CCFE R(15)26
- [3] Vladimirov P V and Moeslang A 2004 *J. Nucl. Mater.* **329** 233 7
- [4] Vladimirov P V and Borodin V A 2017 *Nucl. Instrum. Methods Phys. Res. B* **393** 195 9
- [5] Sublet J C, Eastwood J W and Morgan J G 2014 The FISPACT II User Manual *Tech. Rep.* CCFE R(11)11 CCFE Issue 6
- [6] Norgett M J, Robinson M T and Torrens I M 1975 *Nucl. Eng. Des.* **33** 50 4
- [7] Stoller R E, Nordlund K and Malerba L Displacement cascade damage production in metals *State of the Art Report on Structural Materials Modelling* NEA/NSC/R(2016)5 p 68
- [8] Ziegler J F, Biersack J P and Ziegler M D 2008 *SRIM The Stopping and Range of Ions in Matter* (Chester, MD: SRIM Co.) (<http://srim.org>)
- [9] Mohammadi A, Hamidi S and Asadabad M A 2017 *Nucl. Instrum. Methods Phys. Res. B* **412** 19 27
- [10] Borodin V A and Vladimirov P V 2016 *Nucl. Mater. Energy* **9** 216 20
- [11] Nordlund K, Ghaly M, Averbach R S, Caturla M, Diaz de la Rubia T and Tarus J 1998 *Phys. Rev. B* **57** 7556 70
- [12] Stoller R E and Greenwood L R 1999 *J. Nucl. Mater.* **271** & **272** 57 62
- [13] Bacon D J, Osetsyky Y N, Stoller R and Voskoboinikov R E 2003 *J. Nucl. Mater.* **323** 152 62
- [14] Stoller R E and Calder A F 2000 *J. Nucl. Mater.* **283** 287 746 52
- [15] Stoller R E, Toloczko M B, Was G S, Certain A G, Dwaraknath S and Garner F A 2013 *Nucl. Instrum. methods Phys. Res. B* **310** 75 80
- [16] Nordlund K, Wallenius J and Malerba L 2006 *Nucl. Instrum. Methods Phys. Res. B* **246** 322 32
- [17] Jackson M L, Fossati P C M and Grimes R W 2016 *J. Appl. Phys.* **120** 045903
- [18] Malerba L 2006 *J. Nucl. Mater.* **351** 28 38
- [19] Stoller R E 2012 *Comprehensive Nuclear Materials* ed R J M Konings *et al* (Amsterdam: Elsevier) pp 293 332
- [20] Zarkadoula E, Daraszewicz S L, Duffy D M, Seaton M A, Todorov I T, Nordlund K, Dove M T and Trachenko K 2014 *J. Phys.: Condens. Matter* **26** 085401
- [21] Zarkadoula E, Daraszewicz S L, Duffy D M, Seaton M A, Todorov I T, Nordlund K, Dove M T and Trachenko K 2013 *J. Phys.: Condens. Matter* **25** 125402
- [22] Zarkadoula E, Duffy D M, Nordlund K, Seaton M A, Todorov I T, Weber W J and Trachenko K 2015 *J. Phys.: Condens. Matter* **27** 135401
- [23] Broeders C H M and Konobeev A Y 2005 *J. Nucl. Mater.* **336** 201 9
- [24] Brailsford A D and Bullough R 1981 *Phil. Trans. R. Soc. A* **302** 87 137
- [25] Borodin V A 1994 *Physica A* **211** 279 316
- [26] Björkas C, Juslin N, Timko H, Vörtler K, Nordlund K, Henriksson K and Erhart P 2009 *J. Phys.: Condens. Matter* **21** 445002
- [27] Ganchenkova M G and Borodin V A 2007 *Phys. Rev. B* **75** 054108
- [28] Ganchenkova M G, Vladimirov P V and Borodin V A 2009 *J. Nucl. Mater.* **386** 388 79 81